Grid Scale Effects on Watershed Soil Erosion Models

Rosalia Rojas[1]; Mark Velleux[2]; Pierre Y. Julien, M.ASCE[3]; and Billy E. Johnson[4]

Abstract: The model CASC2D-SED was applied to the Goodwin Creek experimental watershed in Mississippi to define erosion model response to raster-based grid cell sizes. The model was parameterized at a 30 m grid, then calibrated and validated to three representative thunderstorms. The simulated hydrographs replicated the measurements of peak discharge, runoff volume, and time to peak. The model also calculated sediment yields within ±50% of the field measurements. Resampling the watershed digital elevation model at scales from 30 m to 330 m reduced the land surface slopes and changed the channel topology. In general, very good modeling results are obtained at grid sizes of 30 m and 90 m, which is comparable to the plot sizes of the universal soil loss equation. At grid sizes coarser than 150 m, the sediment source areas became less appropriately depicted and the calculated sediment delivery ratios became unrealistically high. Grid sizes smaller than 150 m are recommended for proper watershed simulation of upland erosion and sediment yield.

DOI: 10.1061/(ASCE)1084-0699(2008)13:9(793)

CE Database subject headings: Soil erosion; Hydrologic models; Sediment; Watersheds; Mississippi.

Introduction

Land surface erosion models should describe the physical processes that control erosion using parameters that directly relate to measurable physical soil properties (Lane et al. 1988). In general, upland erosion losses are influenced by spatial variations in topography, vegetation, soil types, and land use. This heterogeneity is further influenced by the redistribution of soil particles during runoff events, which drives long-term landscape change and in turn affects the hydrological processes acting on individual hillslopes (Brooks and McDonnell 2000). Consequently, the parameterization and accuracy of watershed models depends on the spatial scale or cell size of soil erosion models. Several studies of the effect of grid size have been carried out (Quinn et al. 1991; Zhang and Montgomery 1994; Wolock and Price 1994; Beven 1995; Bruneau et al. 1995; De Roo 1996; Saulnier et al. 1997; Yu 1997; Wang et al. 2000). As cell size decreases, model accuracy can be gained, up to the limit of accuracy of underlying data.

When using the universal soil loss equation (USLE), grid size correction factors have been defined (Julien and Frenette 1987; Julien and González del Tanago 1991). When using a large digital elevation model (DEM), Molnar and Julien (1998, 2000) also defined a range of conditions where the USLE model could be used. Models based on the USLE, however, cannot describe the internal dynamics of the physical interactions between erosion on steep hillslopes and deposition on flat areas like floodplains. It seems rather promising to use dynamic models describing sheet erosion processes from rainstorms and to examine the erosion and transport of sediment from the upland sources to the outlet of a watershed. The possibility of simulating rainfall events on well instrumented natural watersheds clearly deserves attention and should contribute to new developments in this field.

Spatially distributed models such as CASC2D-SED (Julien et al. 1995; Johnson et al. 2000; Rojas 2002; Julien and Rojas 2002) are of particular interest in this context. Spatially distributed models have the ability to represent the landscape on fine spatial scales. This allows a detailed representation of the natural heterogeneity of land surface and soil erosion characteristics. The computational effort required to generate a solution also depends on grid size. For example, a simulation at a 30 m scale will have four times as many cells and will also require about half the time step of a 60 m simulation. This corresponds to about an order of magnitude increase in computational effort and database management compared to a simulation at a 60 m scale. While a reduced spatial resolution increases computational speed, it comes at the potential cost of reduced model accuracy. The tradeoff between cell size and computational effort in watershed erosion models is, therefore, examined in this article.

The objective of this article is to examine grid size effects on numerical modeling of upland erosion and sediment yield from natural watersheds. The approach was to calibrate and validate the model CASC2D-SED for the simulation of water and sediment transport for three representative thunderstorms on the Goodwin Creek experimental watershed at a 30 m grid scale. The procedure was then repeated at five additional grid scales: 90, 150, 210, 270, and 330 m for a thorough comparison of model results. The analysis concludes with a recommendation of appropriate grid sizes for erosion models at the watershed scale.

Overview of CASC2D-SED

CASC2D-SED is a physically based, spatially distributed watershed model that can simulate the hydrologic and sediment trans-

[1]Research Associate, Dept. of Civil and Environmental Engineering, Colorado State Univ., Fort Collins, CO 80523–1320. E-mail: rosalia@sierranieves.com

[2]Senior Project Manager, HydroQual, Inc., 1200 MacArthur Blvd., Mahwah, NJ 07430. E-mail: mvelleux@hydroqual.com

[3]Professor, Dept. of Civil and Environmental Engineering, Colorado State Univ., Fort Collins, CO 80523–1320. E-mail: pierre@engr.colostate.edu

[4]Research Hydraulic Engineer, U.S. Army Corps of Engineers, Engineer Research and Development Center, Vicksburg, MS 39180.

Note. Discussion open until February 1, 2009. Separate discussions must be submitted for individual papers. The manuscript for this paper was submitted for review and possible publication on August 30, 2006; approved on December 6, 2007. This paper is part of the ***Journal of Hydrologic Engineering***, Vol. 13, No. 9, September 1, 2008. ©ASCE, ISSN 1084-0699/2008/9-793–802/$25.00.

port response of a watershed subject to a distributed rainfall field for a single event (Johnson et al. 2000; Rojas 2002; Julien and Rojas 2002). Major hydrologic processes vary in time and space to describe precipitation, interception, infiltration, Hortonian (infiltration excess) overland flow, overland soil erosion and deposition, sediment delivery to the stream channel network, channel flow routing, and channel sediment erosion and deposition. Sheet and rill erosion from upland areas delivers solids to the stream network. These solids are transported as washload or bed-material load depending on hydraulic conditions and grain size. Solids deposited on the channel bed during a simulation can be resuspended depending on hydraulic conditions. A review of the flow, upland erosion, and channel sediment transport capacity relationships in CASC2D-SED follows. Detailed descriptions of all CASC2D-SED hydrologic and sediment transport algorithms are provided by Johnson et al. (2000), Rojas (2002), and Julien and Rojas (2002). A brief presentation of the key components of the model follows.

During rainstorms, the rainfall intensity in excess of the infiltration rate causes ponding of surface water. Overland flow occurs when the ponded water depth exceeds the depression storage of the upland area. Overland flow is governed by conservation of mass and momentum as expressed by the vertically integrated diffusive wave approximation to the St. Venant equations in two dimensions (Julien 2002)

$$\frac{\partial h}{\partial t} + \frac{\partial q_x}{\partial x} + \frac{\partial q_y}{\partial y} = i_n - f = i_e \tag{1}$$

$$q_x = \alpha_x h^{\beta} \tag{2a}$$

$$q_y = \alpha_y h^{\beta} \tag{2b}$$

$$\alpha_x = \frac{|S_{fx}|^{1/2}}{n} \tag{3a}$$

$$\alpha_y = \frac{|S_{fy}|^{1/2}}{n} \tag{3b}$$

$$S_{fx} = S_{0x} - \frac{\partial h}{\partial x} \tag{4a}$$

$$S_{fy} = S_{0y} - \frac{\partial h}{\partial y} \tag{4b}$$

where h=surface water depth [L]; q_x, q_y=unit discharge in the x or y direction=Q_x/B_x, Q_y/B_y [L^2/T]; Q_x, Q_y=flow in the x or y direction [L^3/T]; B_x, B_y=flow width in the x or y direction [L]; i_n=net precipitation (gross precipitation minus interception) rate [L/T]; f=infiltration rate [L/T]; i_e=excess precipitation rate [L/T]; α_x, α_y=resistance coefficient for flow in the x or y direction [$L^{1/3}/T$]; β=resistance exponent for turbulent flow=5/3 [dimensionless]; n=Manning roughness coefficient (SI units) [$T/L^{1/3}$]; S_{fx}, S_{fy}=friction slope (energy grade line) in the x or y direction [dimensionless]; and S_{0x}, S_{0y}=land surface slope in the x or y direction [dimensionless].

Channel flow is also governed by conservation of mass and momentum as expressed by the diffusive wave approximation of the St. Venant equation (Julien et al. 1995; Julien 2002) in one dimension along the channel in the down-gradient "x" direction

$$\frac{\partial A_c}{\partial t} + \frac{\partial Q_x}{\partial x} = q_l \tag{5}$$

$$Q_x = \frac{1}{n} A_c R_h^{2/3} |S_{fx}|^{1/2} \tag{6}$$

where A_c=cross-sectional area of flow [L^2]; Q_x=total discharge [L^3/T]; q_l=lateral flow into the channel [L^2/T]; R_h=hydraulic radius of flow=A_c/P_e [L]; and P_e=wetted perimeter of flow ['L]. The friction slope in the direction of flow depends on the channel bed slope (S_{0x}) and water surface gradient (dh/dx) as given by Eq. (4a).

Upland erosion is computed by size fraction for sands, silts, and clays based on transport capacity using a modified form of the Kilinc and Richardson (K-R) (1973) equation. The K-R equation was developed to estimate the sheet and rill erosion from bare sand soils and was extended to consider more general cases of soil erosion by including USLE terms (Julien 1995)

$$q_s = 23{,}210 S_f^{1.664} q^{2.035} \frac{K}{0.15} CP \tag{7}$$

where q_s=unit sediment discharge (tons $m^{-1}\,s^{-1}$) [M/LT]; S_f=friction slope (in the x or y direction) [dimensionless]; q=unit discharge (in the x or y direction) ($m^2\,s^{-1}$) [L^2/T]; and K, C, and P are the USLE soil erodibility (tons/acre) [M/L], land-use management factor [dimensionless], and conservation practice factor [dimensionless], respectively. Note that Eq. (7) depends on land surface slope and unit discharge. As described by Julien and Simons (1985) and Prosser and Rustomji (2000), soil transport capacity relationships can be reduced to a general form $q_s=kq^{\beta}S^{\gamma}$, where the exponents for flow and slope typically range from approximately 1.0 to 1.8 with median values of 1.4. The original K-R relationship has been used in this study; however, CASC2D-SED could easily accommodate different values of these exponents if needed.

Bed sediment erosion through stream channels is computed based on transport capacity using the Engelund and Hansen (1967) total load equation

$$C_w = 0.05\left(\frac{G_s}{G_s - 1}\right)\frac{vS_f}{\sqrt{(G_s-1)gd_s}}\sqrt{\frac{R_h S_f}{(G_s-1)d_s}} \tag{8}$$

$$q_s = Q_x C_w / R_h \tag{9}$$

where C_w=sediment concentration by weight [dimensionless]; G_s=sediment specific gravity [dimensionless]; v=channel flow velocity [L/T]; S_f=friction slope [dimensionless]; g=gravitational acceleration [L/T^2]; d_s=particle diameter [L]; and R_h=hydraulic radius [L]. Note that Eq. (8) depends on friction slope and flow velocity in the main channel.

Application to Goodwin Creek

Goodwin Creek is operated by the Agricultural Research Service (ARS) National Sedimentation Laboratory (NSL), and is organized and instrumented for conducting extensive research on watershed hydrology, upstream erosion, and instream sediment transport (Blackmarr 1995; Alonso 1996). The watershed has a database with precipitation, runoff, and sediment measurements at several locations from 1981 through 1996 (and more recently through 2002).

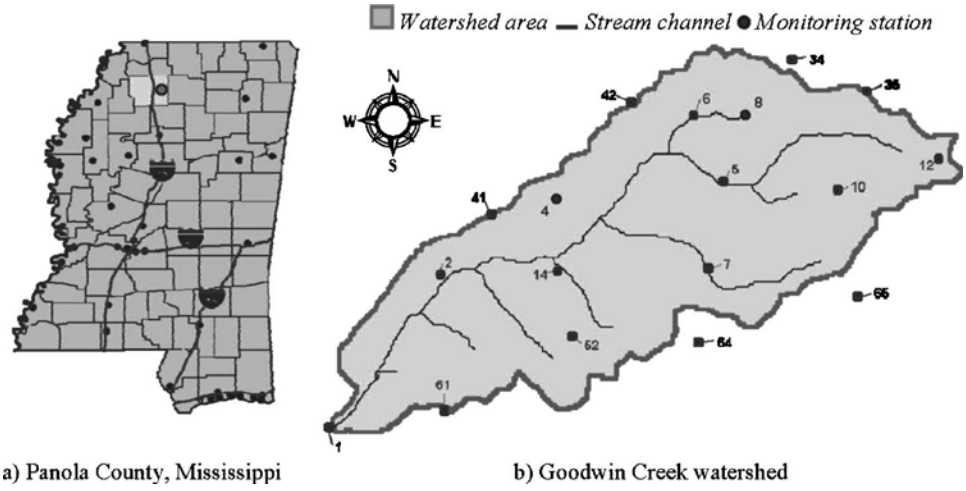

Fig. 1. Goodwin Creek watershed location

Site Description

The watershed, channel network, monitoring station locations are presented in Fig. 1. The watershed is 21.4 km^2 with land surface elevations that range from 71 to 128 m above mean sea level and an average channel bed slope of 0.004. Two major soil groups are found on this watershed. The Collins-Fallaya-Grenada-Calloway associations are poorly to moderately well drained, silty soils that cover most of the cultivated area in the watershed. The Loring-Grenada-Memphis associations are well to moderately well drained, silt loam soils on gently sloping to very steep terrain that cover most pasture and wooded areas. Approximately 14% of the watershed is cultivated, 26% forested, and 60% pasture or grassland. Further description of the watershed is provided by Blackmarr (1995).

Model Setup, Calibration, and Validation

CASC2D-SED requires geospatial data input as raster maps (square grid cells). A 30 m grid scale was selected as the basis for model calibration and subsequent assessments of grid scale impacts on erosion estimates. The 30 m grid scale was chosen for two primary reasons: (1) it was the native resolution of the source DEM (and is a commonly available resolution in standard repositories such as the USGS National Elevation Dataset); and (2) this scale is close to the standard 22.1 m (72.6 ft) plot size used to develop the USLE. Use of the DEM at its native resolution also reduces potential differences in simulation results due to data processing.

Watershed topography is represented using DEM data to define watershed area, land surface elevations and slopes, as well as channel network topology. DEM data for the watershed at a 30 m spatial resolution as obtained from the ARS-NSL are presented in Fig. 2. Stream channel characteristics (width, bank height, etc.) were determined from surveys completed by the ARS (Blackmarr 1995). Surface soil and land-use maps for the watershed are also presented in Fig. 2. Soils data, particularly texture (grain size distribution), were used to estimate soil infiltration properties (saturated hydraulic conductivity, capillary head, etc.) and erosion characteristics, particularly USLE erodibility (K) factors. Interception depth, overland roughness coefficient, and USLE cover (C) and practice (P) factors were derived from the land-use data.

Consistent with the work of Johnson et al. (2000), the October 17, 1981 storm event was used for model calibration. The model was validated for two additional events: August 28, 1982 and September 20, 1983. The validation events were significantly different from the calibration event in terms of the spatial distribution of rainfall, maximum rainfall intensities, and antecedent moisture conditions. Precipitation measurements from 16 rain gages within and immediately adjacent to the watershed were used to define the model rainfall time series. Within the model, spatially distributed estimates of rainfall are calculated by interpolating point rainfall rate measurements using an inverse distance weighting algorithm. A summary of rainfall conditions for these events is presented in Table 1.

Model Calibration and Validation Results

Subject to physical constraints corresponding to soil texture, land use, and antecedent moisture conditions (Rawls et al. 1983; Saxton et al. 1986; Woolhiser 1975; Wischmeier and Smith 1978), the main calibration parameters were the saturated hydraulic conductivity (K_s), flow resistance (Manning n), and soil erodibility (K). The initial soil moisture deficit for each event was estimated from antecedent rainfall. Model parameter values are summarized in Tables 2 and 3.

Simulated and measured flow and sediment discharges at the watershed outlet (Station 1) and two additional sites (Stations 4 and 7) for the calibration and validation events are presented (Figs. 3 and 4). Results for other stations are summarized by Rojas (2002). The model reproduced discharge volume, peak discharge, and time to peak at the watershed outlet. Results for other locations are more variable but generally capture the timing and magnitude of flow and sediment discharges. Simulated sediment yields for all monitoring stations are within approximately $\pm 50\%$ of measured values (Fig. 5). The simulated net sediment accumulation (deposition minus erosion) across the watershed for the calibration event is shown in Fig. 6. The sediment rating curves for the three events modeled are shown along with measured conditions for the period of record (through 1996) in Fig. 7.

Some differences between simulated and measured flow conditions may be attributable to the uncertainty in the spatial interpolation of rainfall estimates from point measurements because rainfall patterns at different gages are not highly correlated. For sediments, some differences may be attributable to spatial variability in soil types from the GIS maps as well as spatial temporal variability in land use such as the seasonal changes in land cover

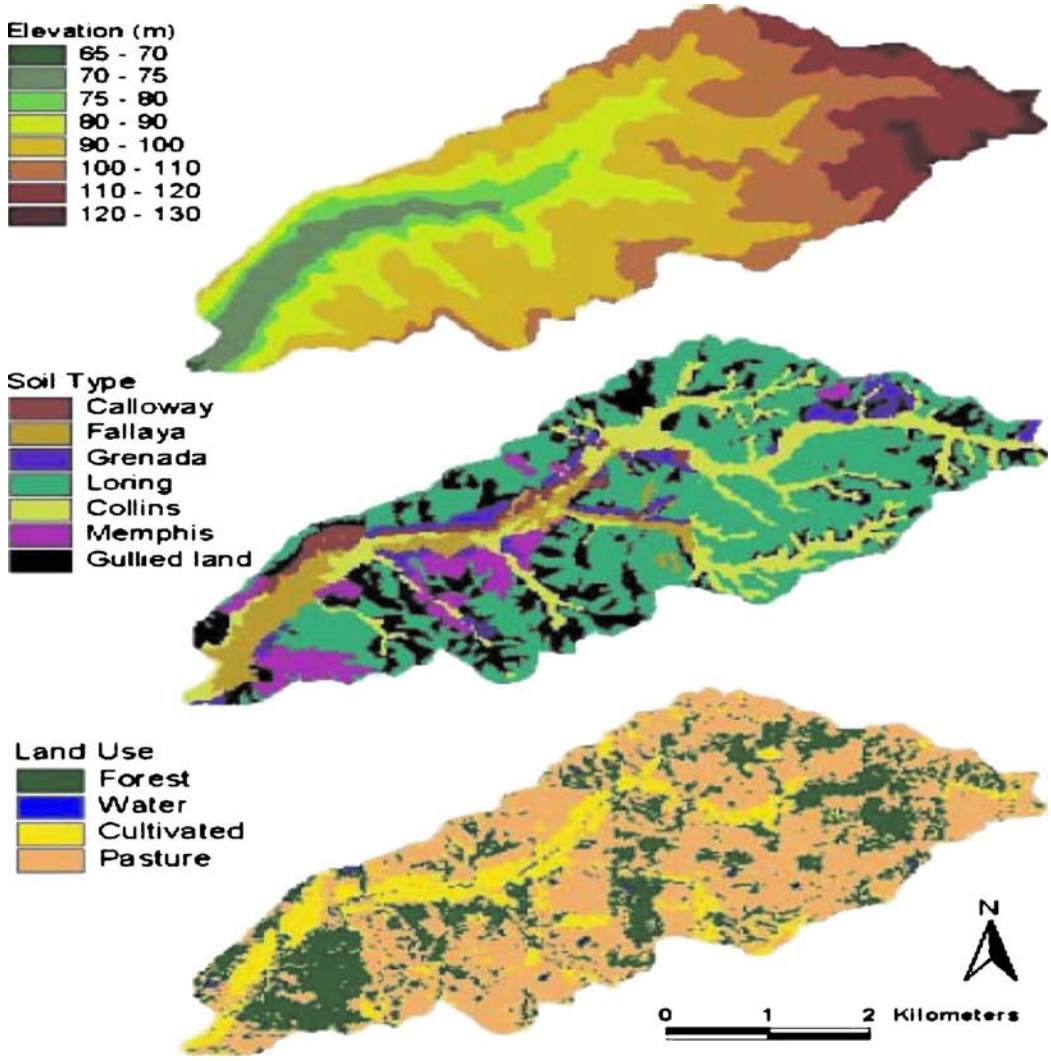

Fig. 2. Goodwin Creek elevation (DEM), soil type, and land-use data (30-m resolution)

for cultivated and pasture areas. However, the numerous hydraulic and sediment monitoring stations had fixed-elevation concrete bases that limited channel erosion losses from within Goodwin Creek. Overall, the events simulated demonstrate that the model calibration is robust and yields results that replicate very well the rapid changes in water and sediment discharge for these short flash floods. The results are representative of typical storm events in the historical period of record (Fig. 7) and provide an appropriate basis for analysis of model grid scale effects.

Table 1. Rainfall Characteristics for Calibration and Validation Events

Event	Calibration Oct. 17, 1981	Validation Aug. 28, 1982	Validation Sept. 20, 1983
Rainfall duration [hour]	4.8	9.8	6
Mean rainfall depth [mm]	73.6	147.5	61.7
Rainfall depth range[a] [mm]	66.0–78.7	135.4–154.9	39.1–91.7
Mean rainfall intensity [mm/h]	14.7	10.1	10.3
Rainfall intensity range[a] [mm/h]	0–51.6	0–65.5	0–90.3

[a]As measured at any gage during the rainfall event.

Effects of Model Grid Scale

To examine the impact of grid scale on erosion calculations, the Goodwin Creek 30 m DEM was resampled to five upscaled spatial resolutions: 90, 150, 210, 270, and 330 m. Soil type and land use were also resampled at each upscaled grid resolution. The process of cell aggregation alters the representation of land surface and channel network characteristics. This affects subsequent surface hydrology and soil erosion calculations (Refsgaard 1997; Thieken et al. 1999; Kuo et al. 1999; Wolock and McCabe 2000; Vázquez et al. 2002). It is interesting to note that Schoorl et al. (2000) used an artificial DEM where slope did not change as grid size changed. In addition, Kalin et al. (2003) simulated rainfall excess and decoupled overland flow from infiltration. Our approach differs from earlier research in that CASC2D-SED provides direct coupling of surface runoff and infiltration. In addition, the resampling method is applied to a densely instrumented experimental watershed (i.e., Goodwin Creek).

DEM resampling alters the distribution of slopes across the watershed and impacts the definition of the channel network

Table 2. Grain Size Distribution, Infiltration, and Soil Erodibility Values at a 30-m Grid Scale

Soil series	Grain size distribution (%)			K_s (cm/s)	G (cm)	M (cm^3/cm^3)	K
	Sand	Silt	Clay				
Calloway	25	55	20	0.45	28	0.30–0.35	0.4
Fallaya	30	60	10	0.45	28	0.30–0.37	1
Grenada	25	55	20	0.35	20	0.30–0.35	0.4
Loring	25	55	20	0.35	28	0.30–0.32	0.4
Collins	30	60	10	0.22	20	0.30–0.35	0.3
Memphis	25	55	20	0.50	25	0.30–0.33	0.1
Gullied land	25	55	20	0.22	15	0.30–0.38	0.1

Note: K_s=saturated hydraulic conductivity; G=capillary suction head; M=initial soil moisture deficit; and K=soil erodibility.

Table 3. Land-Use Parameter Values at a 30-m Grid Scale

Land use	Roughness (Manning n)	Interception depth (mm)	C	P
Forest	0.25	3	0.001	1
Ponded water	0.01	0	0	1
Cultivated	0.15	1	0.1	1
Pasture	0.2	1.5	0.02	1

(Fig. 8). Steep slopes that occur at finer resolutions are smoothed out at coarser resolutions as discussed in Molnar and Julien (2000). The slope mean and standard deviation also decrease as cell size increases, as shown by Rojas (2002). However, maximum slope values decrease considerably at coarser resolutions. In this analysis, the channel network for each grid resolution was delineated with a constant contributing area threshold to minimize the extent of grid scale impacts caused by differences in stream channel representation. As grid cell size increases and slopes de-

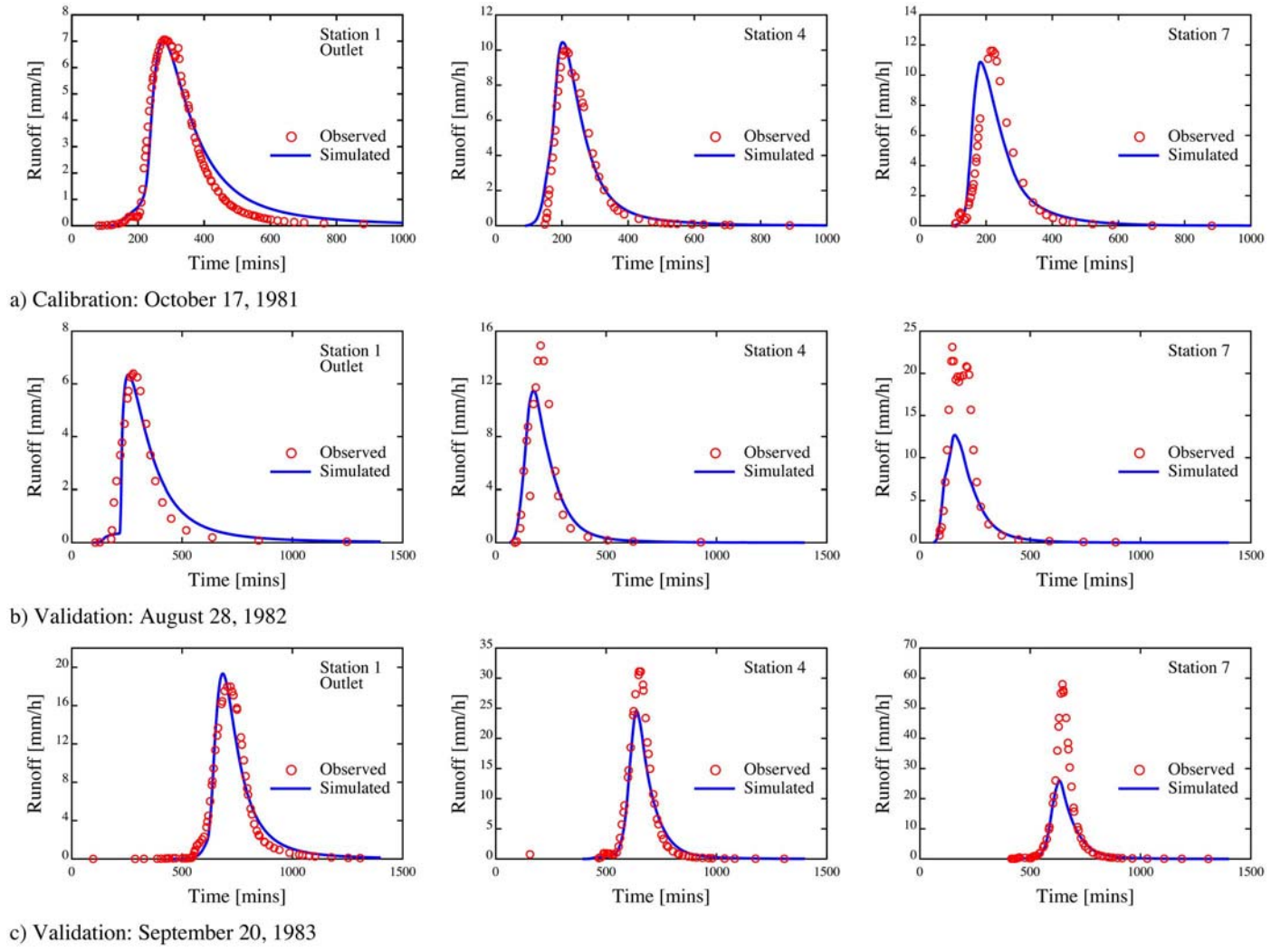

Fig. 3. Simulated and measured water discharge for the model calibration and validation events

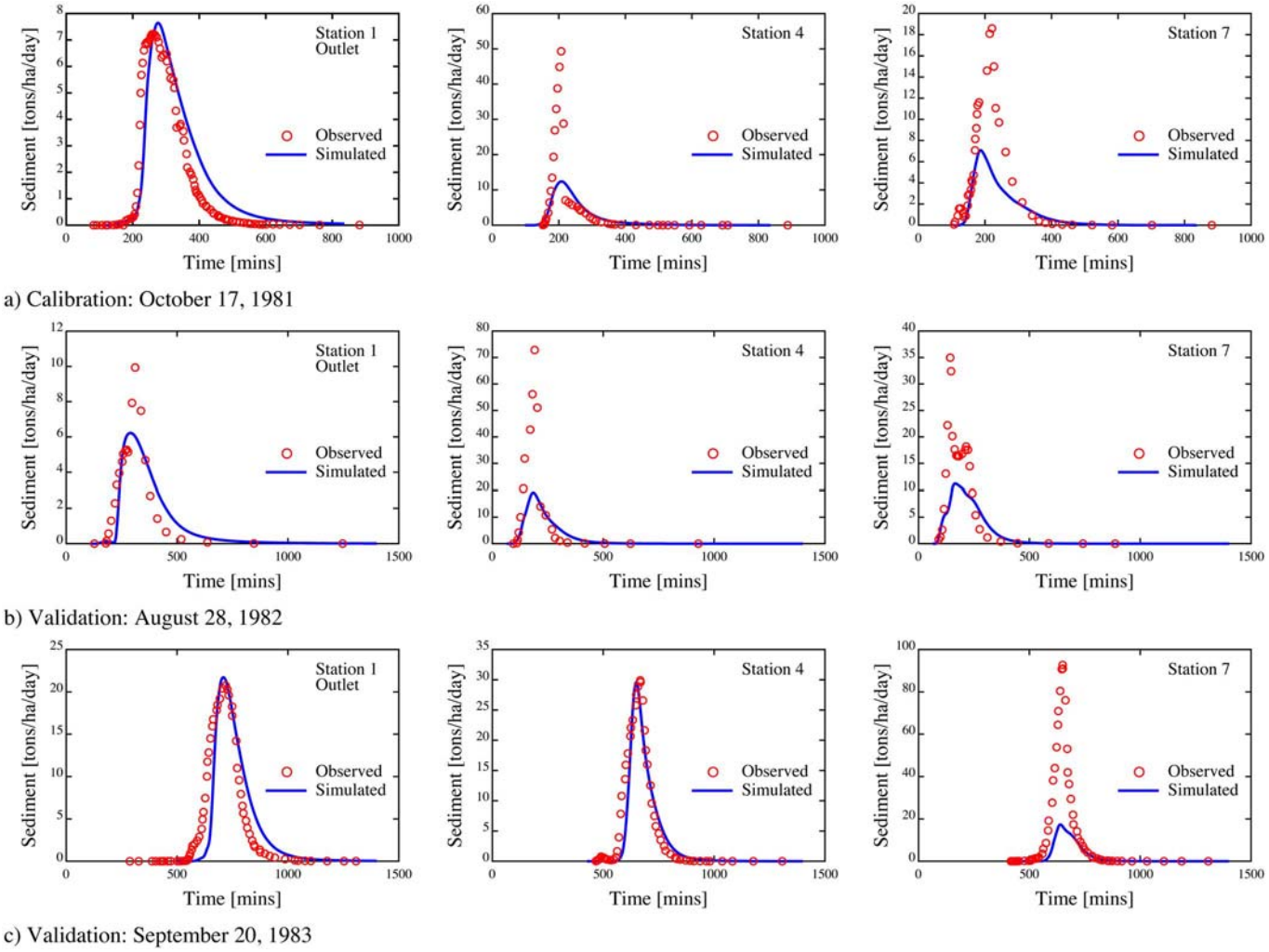

Fig. 4. Simulated and measured sediment discharge for the model calibration and validation events

crease, drainage densities unavoidably decrease from 0.959 to 0.681 km/km^2. In contrast, the area assigned to each soil type and land use in the watershed does not appreciably change with grid resolution (Table 4).

Simulations were conducted for each of the five upscaled grid resolutions using the same hydrological and hydraulic parameters as calibrated for the 30 m grid. Rainfall patterns for the October 17, 1981 storm event were used to examine grid size effects. Additional simulations were also conducted for three uniform rainfall events (Rojas 2002). The results presented here are also representative of those obtained for different storms.

As a result of grid resampling, simulated peak discharges de-

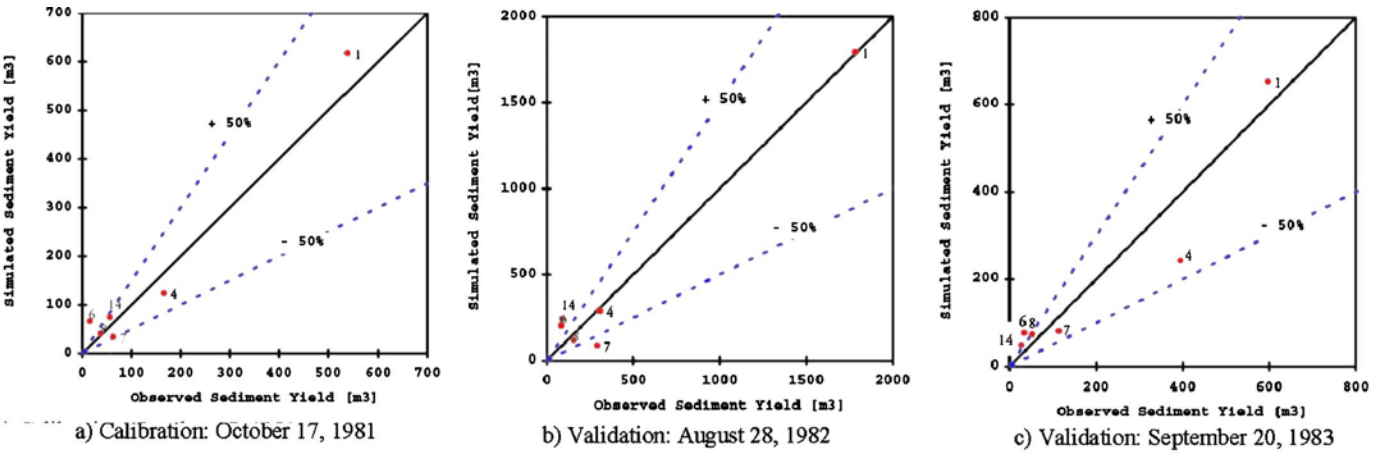

Fig. 5. Simulated and measured sediment yield for the calibration and validation events

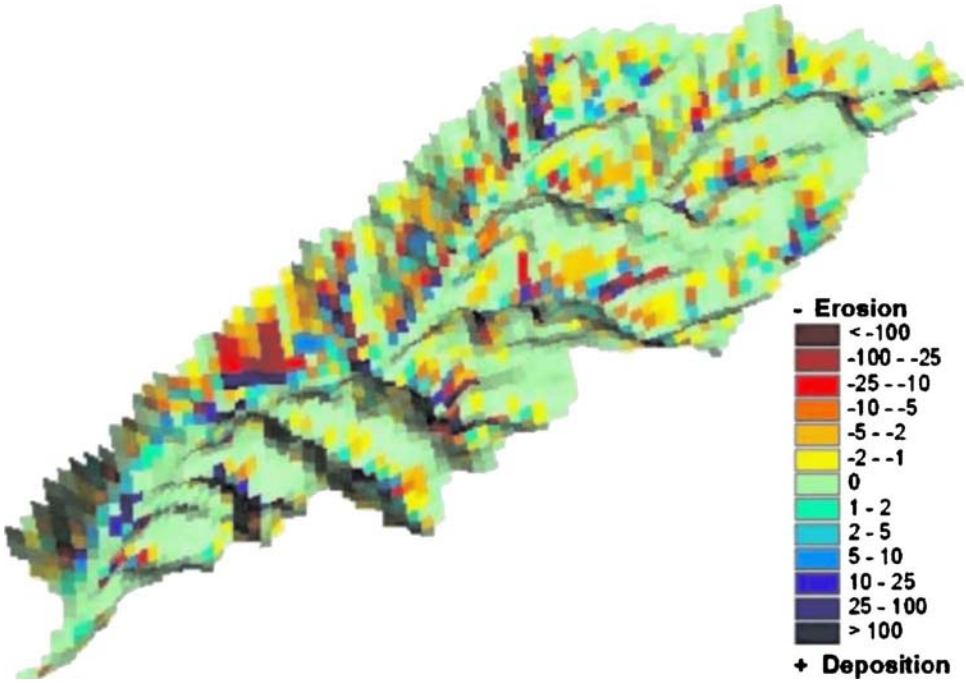

Fig. 6. Net sediment accumulation [tons/ha] for the calibration event

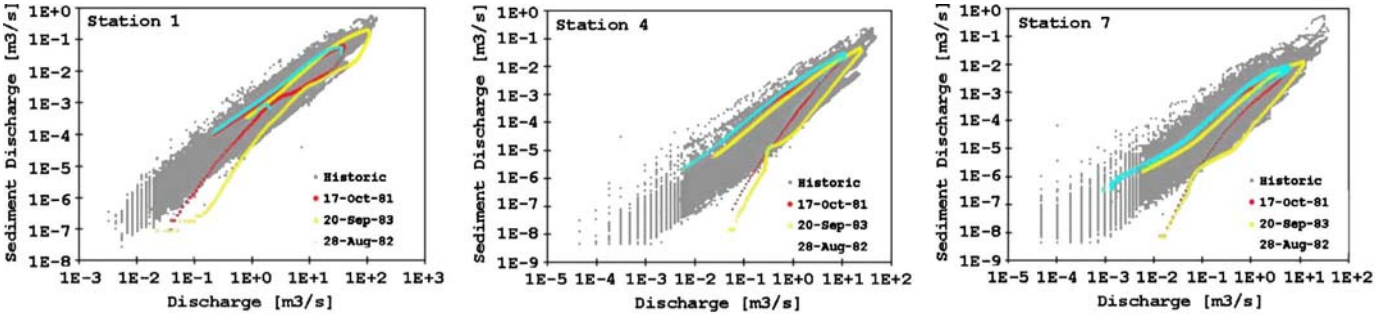

Fig. 7. Simulated and measured sediment rating curves

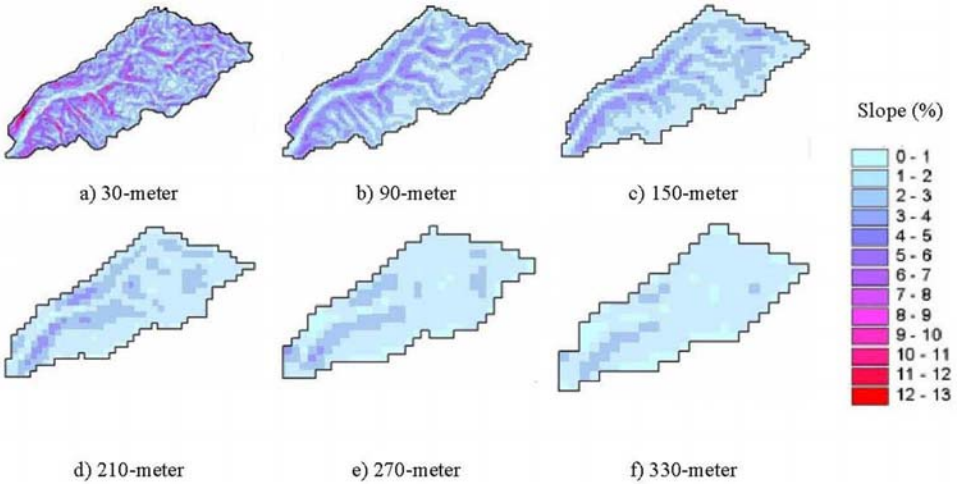

Fig. 8. Land surface slope at six different spatial resolutions from 30 m to 330 m

Table 4. Extent of Soil Type and Land Use for Each Grid Resolution

Grid resolution (m)	Soil type areal extent (%)							Land-use areal extent (%)			
	Calloway	Fallaya	Grenada	Loring	Collins	Memphis	Gullied land	Forest	Water	Cultivated	Pasture
30	2	6	5	47	18	6	16	26	0	14	60
90	2	6	5	46	19	6	16	24	0	12	63
150	3	6	6	46	17	6	16	26	1	14	59
210	2	6	5	48	18	5	16	26	1	18	55
270	3	5	4	47	20	6	14	27	1	12	60
330	3	6	5	49	17	6	13	22	0	16	62

creased and times to peak discharge increased as grid cell sizes increased (Fig. 9). Runoff volumes decreased with increasing grid cell size because a larger portion of the water infiltrated, which in turn reduced the flow unit discharge. These changes to surface runoff substantially altered soil erosion estimates because the underlying soil erosion relationship [Eq. (7)] used in the model is strongly dependent on unit flow discharge (i.e., $q^{2.035}$).

To further isolate the impact of grid resolution on soil erosion estimates, the model calibration parameters were adjusted to maintain equivalent hydrologic responses at all grid scales. This was accomplished by decreasing saturated hydraulic conductivities and initial moisture as needed to reduce infiltration and by increasing channel roughness for increasing grid cell sizes. With these adjustments, the peak discharge, time to peak, and percentages of runoff and infiltration volumes at each upscaled grid resolution were comparable to those obtained at 30 m resolution (Fig. 10).

Discussion and Recommendation

The erosion maps obtained from the model simulations at 30 m to 330 m are shown in Fig. 11. It is quite clear that the results of upland erosion models change with grid size. In particular, the area where erosion is calculated decreases significantly on coarse grids. The best results in this case are obtained at grid sizes finer than 150 m. It is interesting to note that the 30 m results are very close to the range of applicability of the USLE (also the revised USLE—RUSLE). To the extent that USLE parameters (length, slope, K, C, P, etc.) are derived from field measurements on 22.1 m (72.6 ft) standard plot tests, erosion model results are also best at similar grid sizes. Modeling watersheds at grid sizes larger than 150 m is possible; however, the location of the source of sediment can be very important in the analysis of contaminants (Velleux et al. 2006). The example of Fig. 11 clearly illustrates the fact that sediment sources at grid sizes larger than 150 m can be very different from the areas of sediment erosion at 30 m.

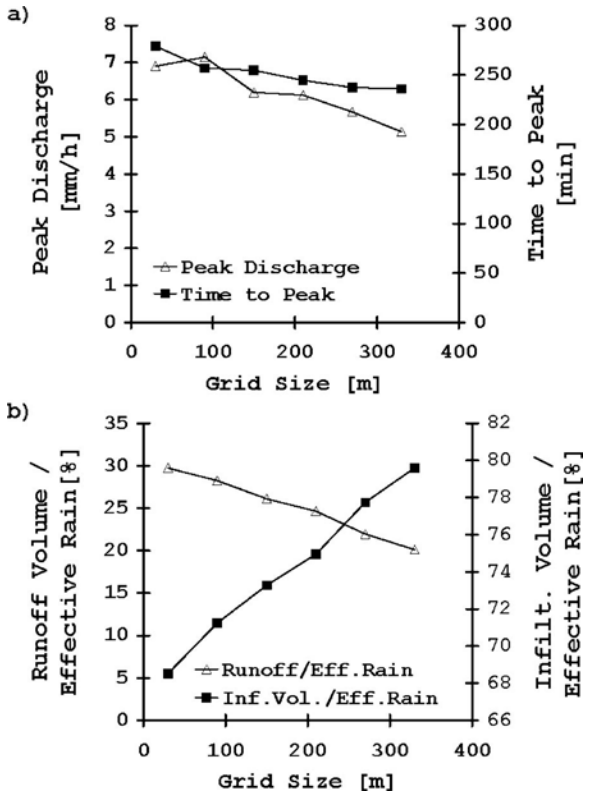

Fig. 9. Unadjusted hydrologic model performance as a function of grid size

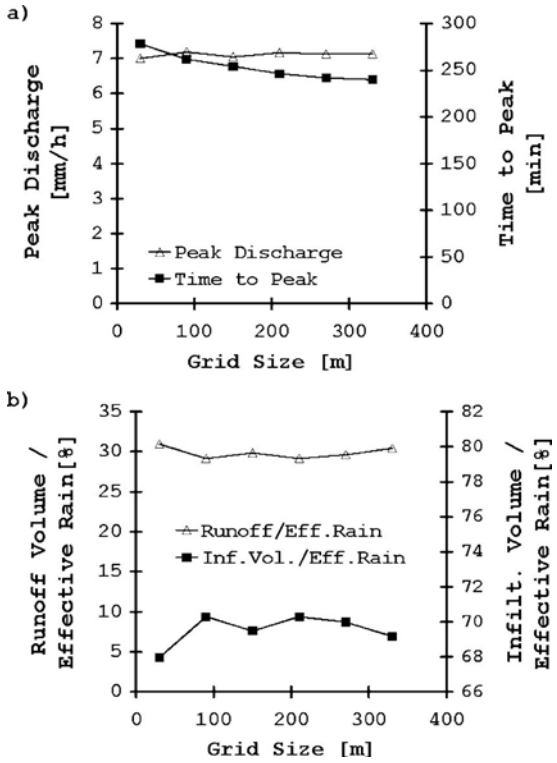

Fig. 10. Adjusted hydrologic model performance at different grid scales

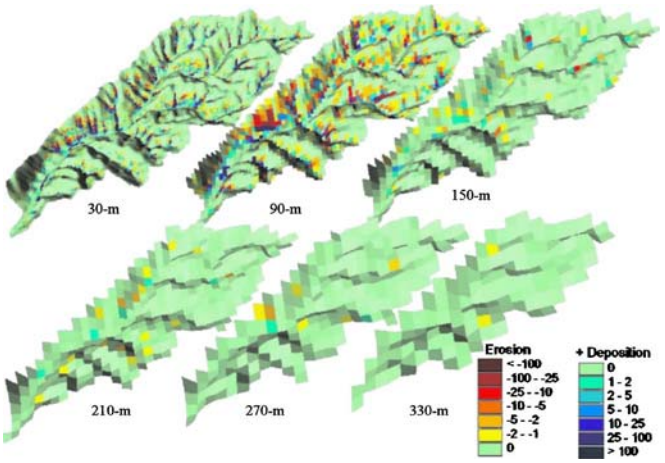

Fig. 11. Spatial distribution of net sediment accumulation [tons/ha] at different grid scales

The CASC2D-SED model also allows easy calculations of the sediment delivery ratio (SDR). The SDR is a ratio of the sediment yield at the outlet to the gross erosion from a watershed. SDR values were computed at the watershed outlet from field data and the upland erosion results for the six grid size simulations. As described by Boyce (1975), the SDR for a 20.5 km^2 (7.9 mi^2) drainage basin ranges from 0.1 to 0.5. Based on CASC2D-SED simulation results, the SDR increased with grid size and ranged from 0.27 to 0.63. Only the 30 and 90 m simulations produced SDR values within the range reported by Boyce, while SDR values for grid sizes 150 m and larger were above the reported range. This SDR analysis thus corroborates our recommendation to use grid sizes finer than 150 m in upland erosion models.

Conclusions

CASC2D-SED was applied to the Goodwin Creek experimental watershed in Mississippi to explore erosion model response for a range of different grid scales. The model was set up, calibrated, and validated at a 30 m grid scale for three typical thunderstorms. Simulated hydrographs were in good agreement with measured total discharge, peak discharge, and time to peak discharge values. Simulated sediment yields varied within ±50% of measured values.

Resampling the Goodwin Creek watershed DEM at different resolutions from 30 m to 330 m reduced the land surface slopes and the channel network topology. Even after adjusting the model parameters to maintain equivalent surface runoff, substantial differences in simulated soil erosion estimates were found at different grid sizes, as shown in Fig. 11. Soil erosion models using parameters from the USLE are best applied at model grid size close to the 22.1 m standard plot size of the USLE. As model grid size increases, the simulated area of soil erosion substantially decreases, and the source areas of upland erosion may not be appropriately defined at grid scales coarser than 150 m. It is thus concluded that the best results to simulate soil erosion can be obtained at grid sizes smaller than 150 m.

Acknowledgments

Financial support was granted through the Instituto Nacional de Investigaciones Agrarias of Spain and the Department of Defense through the Center for Geosciences/Atmospheric Research at Colorado State University, under Cooperative Agreement No. DAAL01-98-2-0078 with the Army Research Laboratory. Goodwin Creek field data were provided courtesy of Carlos Alonso at the USDA-ARS-National Sedimentation Laboratory in Oxford, MS. The collaboration with J. Jorgeson at the Engineer Research and Development Center in Vicksburg, MS, and D. Molnar formerly at Colorado State University has also been greatly appreciated.

Notation

The following symbols are used in this paper:

A_c = cross sectional area of flow [L^2];
B_x, B_y = flow width in the x or y direction [L];
C = cropping-management factor of the USLE [-];
C_w = sediment concentration by weight [-];
d_s = particle diameter [L];
f = infiltration rate [L/T];
G = capillary suction head [L];
G_s = specific gravity of sediment [-];
g = gravitational acceleration [L/T^2];
h = surface water depth [L];
i_n = net precipitation (gross precipitation minus interception) rate [L/T];
i_e = excess precipitation rate [L/T];
K = soil erodibility factor of the USLE (tons/acre) [M/L^2];
K_s = saturated hydraulic conductivity [L/T];
M = initial soil moisture deficit [-];
n = Manning roughness coefficient (SI units) [$T/L^{1/3}$];
P = conservation practice factor of the USLE [-]
P_e = wetted perimeter of flow [L];
Q_x, Q_y = flow in the x or y direction [L^3/T];
Q_x = total discharge [L^3/T];
q = unit discharge (in the x or y direction) ($m^2\ s^{-1}$) [L^2/T];
q_l = lateral flow into the channel [L^2/T];
q_s = unit sediment discharge (tons $m^{-1}\ s^{-1}$) [M/LT];
q_x, q_y = unit discharge in the x or y direction=Q_x/B_x, Q_y/B_y [L^2/T];
R_h = hydraulic radius of flow=A_c/P [L];
S_f = friction slope (in the x or y direction) [-];
S_{fx}, S_{fy} = friction slope (energy grade line) in the x or y direction [-];
S_{0x}, S_{0y} = land surface slope in the x or y direction [-];
v = channel flow velocity [L/T];
α_x, α_y = resistance coefficient for flow in the x or y direction [$L^{1/3}/T$]; and
β = resistance exponent for turbulent flow=$\frac{5}{3}$ [-].

Endnotes

[1]Supporting information that provides detailed descriptions of CASC2D-SED model theory, algorithms, computer code, a user manual, and sample files is available on the Web at: ⟨http://www.engr.colostate.edu/%7Epierre/ce_old/Projects/CASC2D-SED%20Web%20site%20082506/CASC2D-SED-Home.htm⟩. Additional information regarding grid scale effects presented by Rojas (2002) is also available on the web at: ⟨http://www.engr.colostate.edu/%7Epierre/ce_old/Projects/CASC2D-SED%20Web%20site%20082506/RRSDiss4WWW/Dissertation-Index.htm⟩.

References

Alonso, C. V. (1996). "Hydrologic research on the USDA Goodwin Creek experimental watershed, northern Mississippi." *Proc., 16th AGU Hydrology Days*, 25–36, Colorado State Univ., Fort Collins, Colo.

Beven, K. (1995). "Linking parameters across scales: Subgrid parameterizations and scale-dependent hydrological models." *Hydrolog. Process.*, 9(5–6), 507–525.

Blackmarr, W. A. (1995). "Documentation of hydrologic, geomorphic, and sediment transport measurements on the Goodwin Creek experimental watershed, northern Mississippi, for the period 1982–1993—Preliminary release." *USDA-ARS Rep. No. 3* (CD-ROM), U.S. Dept. of Agriculture, Agricultural Research Service, Oxford, Miss.

Boyce, R. (1975). "Sediment routing with sediment delivery ratios." *Proc., Present and Prospective Technology for Predicting Sediment Yields and Sources*, USDA-ARS-S-40, ARS-USDA, Washington, D.C., 61–65.

Brooks, S. M., and McDonnell, R. A. (2000). "Research advances in geocomputation for hydrological and geomorphological modeling towards the twenty-first century." *Hydrolog. Process.*, 14(11–12), 1899–1907.

Bruneau, P., Gascuel-Odoux, C., Tobin, P., Merot, P., and Beven, K. (1995). "Sensitivity to space and time resolution of a hydrological model using digital elevation data." *Hydrolog. Process.*, 9(1), 69–81.

De Roo, A. P. J. (1996). "Soil erosion assessment using GIS." *Geographical information systems in hydrology*, Kluwer, Boston, 339–356.

Engelund, F., and Hansen, E. (1967). *Monograph on sediment transport in alluvial streams*, Teknisk Forlag, Copenhagen, Denmark.

Johnson, B. E., Julien, P. Y., Molnar, D. K., and Watson, C. C. (2000). "The two-dimensional upland erosion model CASC2D-SED." *J. Am. Water Resour. Assoc.*, 36(1), 31–42.

Julien, P. Y. (1995). *Erosion and sedimentation*, Cambridge University Press, New York.

Julien, P. Y. (2002). *River mechanics*, Cambridge University Press, New York.

Julien, P. Y., and Frenette, M. (1987). "Macroscale analysis of upland erosion." *Hydrol. Sci. J.*, 32(3), 347–358.

Julien, P. Y., and González del Tanago, M. (1991). "Spatially varied soil erosion under different climates." *Hydrol. Sci. J.*, 36(6), 511–524.

Julien, P. Y., and Rojas, R. (2002). "Upland erosion modeling with CASC2D-SED." *Int. J. Sediment Res.*, 17(4), 265–274.

Julien, P. Y., Saghafian, B., and Ogden, F. L. (1995). "Raster-based hydrologic modeling of spatially-varied surface runoff." *Water Resour. Bull.*, 31(3), 523–536.

Julien, P. Y., and Simons, D. B. (1985). "Sediment transport capacity of overland flow." *Trans. ASAE*, 28(3), 755–762.

Kalin, L., Govindaraju, R., and Hantush, M. (2003). "Effect of geomorphologic resolution on modeling of runoff hydrograph and sedimentograph over small watersheds." *J. Hydrol.*, 276(1–4), 89–111.

Kilinc, M. Y., and Richardson, E. V. (1973). "Mechanics of soil erosion from overland flow generated by simulated rainfall." *Hydrology Papers No. 63*, Colorado State Univ., Fort Collins, Colo.

Kuo, W. L., et al. (1999). "Effects of grid size on runoff and soil moisture for a variable-source-area hydrology model." *Water Resour. Res.*, 35(11), 3419–3428.

Lane, L. J., Shirley, E. D., and Singh, V. P. (1988). "Modelling erosion on hillslopes." *Modelling geomorphological systems*, M. G. Anderson, ed., Wiley, New York, 287–308.

Molnar, D. K., and Julien, P. Y. (1998). "Estimation of upland erosion using GIS." *Comput. Geosci.*, 24(2), 183–192.

Molnar, D. K., and Julien, P. Y. (2000). "Grid size effects on surface runoff modeling." *J. Hydrol. Eng.*, 5(1), 8–16.

Prosser, I., and Rustomji, P. (2000). "Sediment transport capacity relations for overland flow." *Prog. Phys. Geogr.*, 24(2), 179–193.

Quinn, P., Beven, K., Chevallier, P., and Planchon, O. (1991). "The prediction of hillslope flow paths for distributed hydrological modeling using digital terrain models." *Hydrolog. Process.*, 5(1), 59–79.

Rawls, W. J., Brakensiek, D. L., and Miller, N. (1983). "Green-ampt infiltration parameters from soils data." *J. Hydraul. Eng.*, 109(1), 62–70.

Refsgaard, J. (1997). "Parameterisation, calibration and validation of distributed hydrological models." *J. Hydrol.*, 198(1–4), 69–97.

Rojas, R. (2002). "GIS-based upland erosion modeling, geovisualization, and grid size effects on erosion simulations with CASC2D-SED." Ph.D. thesis, Dept. of Civil Engineering, Colorado State Univ., Fort Collins, Colo.

Saulnier, G.-M., Obled, C., and Beven, K. (1997). "Analytical compensation between DTM grid resolution and effective values of saturated hydraulic conductivity within the TOPMODEL framework." *Hydrolog. Process.*, 11(9), 1331–1346.

Saxton, K., Rawls, W., Romberger, J., and Papendick, R. (1986). "Estimating generalized soil-water characteristics from texture." *Soil Sci. Soc. Am. J.*, 50(4), 1031–1036.

Schoorl, J. M., Sonneveld, M. P. W., and Veldkamp, A. (2000). "Three-dimensional landscape process modelling: The effect of DEM resolution." *Earth Surf. Processes Landforms*, 25(9), 1025–1034.

Thieken, A. H., Lücke, A., Diekkrüger, B., and Richter, O. (1999). "Scaling input data by GIS for hydrological modelling." *Hydrolog. Process.*, 13(4), 611–630.

Vázquez, R. F., Feyen, L., Feyen, J., and Refsgaard, C. (2002). "Effect of grid size on effective parameters and model performance of the MIKE-SHE code." *Hydrolog. Process.*, 16(2), 355–372.

Velleux, M., Julien, P. Y., Rojas-Sanchez, R., Clements, W., and England, J. (2006). "Simulation of metals transport and toxicity at a mine-impacted watershed: California Gulch Colorado." *Environ. Sci. Technol.*, 40(22), 6996–7004.

Wang, M., Hjelmfelt, A. T., and Garbrecht, J. (2000). "DEM aggregation for watershed modeling." *J. Am. Water Resour. Assoc.*, 36(3), 579–584.

Wischmeier, W. H., and Smith, D. D. (1978). "Predicting rainfall erosion losses—A guide to conservation planning." *USDA handbook No. 537*, U.S. Dept. of Agriculture in cooperation with Purdue Agricultural Experiment Station.

Wolock, D. M., and McCabe, G. J. (2000). "Differences in topographic characteristics computed from 100- and 1,000-m resolution digital elevation model data." *Hydrolog. Process.*, 14(6), 987–1002.

Wolock, D. M., and Price, C. V. (1994). "Effects of digital elevation model map scale and data resolution on a topography-based watershed model." *Water Resour. Res.*, 30(11), 3041–3052.

Woolhiser, D. A. (1975). "Simulation of unsteady overland flow." *Unsteady flow in open channels*, K. Mahmood and V. Yevjevich, eds., Water Resources Publications, Fort Collins, Colo.

Yu, Z. (1997). "Grid-spacing effect on watershed hydrologic simulations." *Hydrol. Sci. Technol.*, 13(1–4), 75–85.

Zhang, W., and Montgomery, D. R. (1994). "Digital elevation model grid size, landscape representation, and hydrologic simulations." *Water Resour. Res.*, 30(4), 1019–1028.